Biomaterials and Biomechanics in Bioengineering, *Vol. 4, No. 1 (2019) 21-32*
DOI: https://doi.org/10.12989/bme.2019.4.1.021

Hydroxyapatite prepared from eggshell and mulberry leaf extract by precipitation method

Shih-Ching Wu[1a], Hsueh-Chuan Hsu[1], Shih-Kuang Hsu[1], Mei-Yi Liu[2] and Wen-Fu Ho[*2]

[1]Department of Dental Technology and Materials Science, Central Taiwan University of Science and Technology, 666, Buzih Rd., Beitun District, Taichung 40601, Taiwan
[2]Department of Chemical and Materials Engineering, National University of Kaohsiung, Kaohsiung, 700 Kaohsiung University Rd., Nanzih District, Kaohsiung 81148, Taiwan

(Received June 10, 2018, Revised March 2, 2019, Accepted March 5, 2019)

Abstract. Eggshell is a waste material after the usage of egg. In this work, biowaste chicken eggshells were used for preparing carbonated hydroxyapatite (HA) nanoparticles of high purity through aqueous precipitation method at room temperature. The eggshell-derived HA will be a cost-effective bioceramics for biomedical applications and an effective material-recycling technology. Additionally, mulberry leaf extract was used as a template to regulate the morphology, size and crystallinity of HA, and the effects of pH value were also examined. Characterization of the samples was performed by X-ray diffraction (XRD) and Fourier transform infrared (FT-IR) spectroscopy. Scanning electron microscopy (SEM) was used to determine the size, shape and morphology of HA. The results indicate that only one phase of HA were synthesized in the both absence and presence of mulberry leaf extract at pH of 7 and above, while DCPD or DCPA/DCPD phase was observed at pH 4 condition. The crystallite sizes of the HA samples obviously decreased when adding mulberry leaf extract as a template, while they decreased gradually as the solution pH levels increased. With increasing pH level from 7 to 14, the rod-like HA nanoparticles gradually changed to spherical shape at pH 14. Note that, the obtained product is Mg and Sr containing A- and B-type carbonate HA at alkaline pH and it can be a potential material for biomedical applications.

Keywords: eggshell; mulberry leaf extract; hydroxyapatite; precipitation method; pH value

1. Introduction

Hydroxyapatite (HA, $Ca_{10}(PO_4)_6(OH)_2$), which is the material most similar to the inorganic part of bones and teeth, has been vigorously investigated as implant materials for orthopedic and dental applications due to its excellent bioactivity, osteoconductivity, and osteoinductivity (Best *et al*. 2008). It is also confirmed that HA bioceramics show no toxicity, inflammatory response, pyrogenetic response (Habib *et al*. 2012). Besides, it has also been applied as an adsorbent in environmental protection (Vega *et al*. 2003), for progressing chromatography and other fields (Neira *et al*. 2009). In the past years, several synthesis techniques using a range of different

∗Corresponding author, Professor, E-mail: fujii@nuk.edu.tw
[a]Professor, E-mail: scwu@ctust.edu.tw

http://www.techno-press.org/?journal=bme&subpage=8 ISSN: 2465-9835 (Print), 2465-9959 (Online)

reactants (Ca and P) have been developed for preparing HA powders, including solid state reactions, aqueous precipitation, sol-gel, and hydrothermal (Tas 2000, Liu *et al*. 2001, Wu *et al*. 2011, 2013, Ho *et al*. 2013).

Natural bone minerals are nano-structured and non-stoichiometric HA of dimensions 20 nm in diameter and 50 nm long with carbonate. From bionics viewpoint, synthetic apatites to be used for repairing damaged hard tissues are expected to have characteristics closer to those of biological apatite in both composition and structure (Han *et al*. 2002). Nano-sized HA exhibits much enhanced bioactivity and osseointegrative properties than the coarser crystals because of its grain size, large surface area to volume ratio and ultra fine structure similar to biological apatite (Liu *et al*. 2003). Furthermore, the carbonate ion in human bone is in significant amount, from about 3 to 8 wt% (Tadic *et al*. 2002). The carbonated HA has been reported to have appropriate absorbance time periods and good bone formation ability (Matsuura *et al*. 2009).

In the current research, we made an effort to preparing HA powders using eggshells as a calcium source by develop clean, non-toxic and environmentally friendly techniques. The avian eggshell represents 11% of the total weight of the egg and is composed predominantly of calcium carbonate (94%), calcium phosphate (1%), organic matter (4%) and magnesium carbonate (1%) (Krishna *et al*. 2007). Notably, using a synthetic HA containing trace elements (Mg and Sr) as bone substitutes, instead of one without them, would be much beneficial for bone defect healing (Boutinguiza *et al*. 2012).

In this study, aqueous precipitation method was adopted for the fabrication of nano-HA powders with different pH values. The precipitation method is simple, cheap and easy application in industrial production. Moreover, mulberry leaf extract was added as a template. This natural mulberry leaf extract is biodegradable, biocompatible, water soluble and inexpensive in comparison to other biodegradable polymers. Nano-sized HA crystals with controllable size and shape can be synthesized by use of templates (Deng *et al*. 2013). In the present investigation, the synthesized powder was characterized by X-ray diffraction (XRD), scanning electron microscopy (SEM), and Fourier transform infrared (FT-IR) spectroscopy techniques to explore their structural properties.

2. Materials and methods

Biowaste chicken egg shells were firstly cleaned with water and dried overnight at 45℃ in an oven. It was then crushed and powdered using an agate mortar. Afterwards, 2 g of that powder (the calcium carbonate contained in the eggshell is about 94%) was dissolved in 20 ml hydrochloric acid/water solution. For studying the effect of the mulberry leaf extract template on the structure and morphology of synthesized HA, 0.1 g of mulberry leaf extract in 20 ml of the above eggshell solution was prepared and stirred gently but thoroughly. Phosphoric acid (i.e., Ca/P molar ratio = 1.67) was added little by little to the stirred mixture. In whole process, the reaction temperature was kept at 25℃. In order to investigate the effects of pH values on phases of the final product, ammonium hydroxide (NH_4OH) was used to adjust the solution pH at 4, 7, and 10, while KOH was added to adjust the solution pH at 14. Also, for studying the effect of the mulberry leaf extract on the characteristics of synthesized HA, the solution without containing mulberry leaf extract was used as a control. The raw HA materials were obtained by the direct precipitation method at 25℃ for 24 h. After reaction, the as-prepared powders were separated from liquid phase by filtration, rinsed with deionized water, and dried at 45℃ for 24 h. The reactions of HA formation procedures

that occurred are based on the following equations

$$CaCO_3 + 2HCl \rightarrow CaCl_{2(aq)} + CO_2 + H_2O$$
$$10CaCl_{2(aq)} + 20NH_4OH + 6H_3PO_4 \rightarrow Ca_{10}(PO_4)_6(OH)_2 + 20NH_4Cl + 18H_2O$$

X-ray diffraction (XRD; XRD-6000, Shimadzu, Japan) measurements were carried out with CuKα radiation to characterize the crystalline phase of produced powders. The diffractograms were scanned in a 2θ range of 20-50° at a rate of 2°/min. The morphology of the synthetic powders was observed by a field emission scanning electron microscopy (FE-SEM; JSM-7401F, JEOL, Japan). The elemental analysis was carried out using an energy dispersive X-ray spectroscopy (EDS) attached to the SEM. SEM technique was employed to observe the particle size of each synthesized HA powder. For this, the dimensions (length and diameter) of each sample were calculated from measurement of 30 randomly selected individual particles. Fourier transform infrared (FT-IR; FTS-40, Bio-Rad, USA) spectroscopy was performed on finely ground powder within scanning range of 600-4000 cm^{-1} to identify the characteristic peaks of product. In order to evaluate the composition of the synthesized powders and the presence of heavy metals, inductively coupled plasma-atomic emission spectrometry (ICP-AES; 725, Agilent Co., USA) analysis was performed.

The isolate peak (002) plane was used to estimate the crystallite size of HA phase using the well-known Scherrer formula as followed (Fathia *et al*. 2008)

$$X_s = \frac{0.9\lambda}{FWHM\cos\theta} \quad (1)$$

where X_s is the average crystallite size (nm); λ is the X-ray wavelength (1.5406 Å); FWHM is the full-width at half-maximum (rad), and θ (degree) is the Bragg angle related to the diffraction peak under consideration.

From the XRD data, the crystallinity (X_c) of HA nanoparticles was calculated according to the following equation (Landi *et al*. 2000)

$$X_c = 1 - \frac{V_{112/300}}{I_{300}} \quad (2)$$

where I_{300} is the intensity of (300) diffraction peak and $V_{112/300}$ is the intensity of the hollow between (112) and (300) diffraction peaks of HA.

3. Results and discussion

3.1 X-ray diffraction analysis

Fig. 1 shows X-ray diffraction patterns of synthesized powders with and without adding mulberry leaf extract by aqueous precipitation at room temperature under different pH values. In the XRD pattern of the powders prepared without adding mulberry leaf extract after precipitation for 24 h at pH 4, in Fig. 1(a), the crystal structure was detected with mixed phases of dicalcium phosphate dehydrate (DCPD; $CaHPO_4 \cdot 2H_2O$) and dicalcium phosphate anhydrate (DCPA; $CaHPO_4$). When the mulberry leaf extract was added, as shown in Fig. 1(b), DCPD was the major phase prepared in the reaction solution at pH 4. Because the low pH provided limited amount of OH^-, DCPA or DCPD crystals would nucleate and grow in the solution (Sadat-Shojai *et al*. 2012).

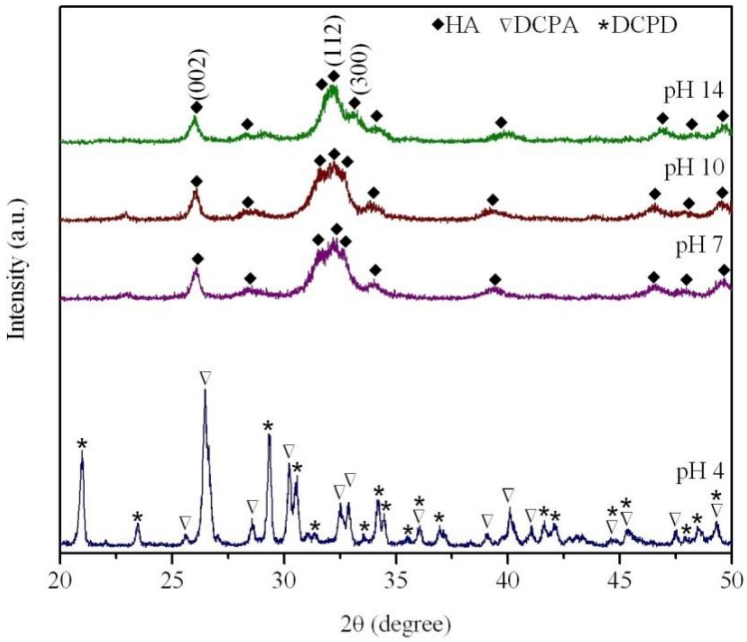

(a) Without adding mulberry leaf extract

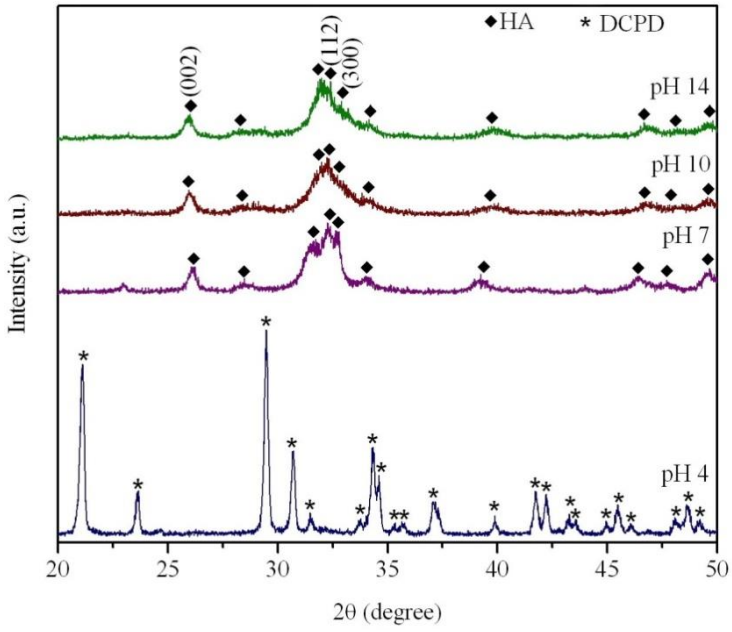

(b) With adding mulberry leaf extract

Fig. 1 XRD patterns of the synthesized powders by aqueous precipitation at room temperature under different pH values

It has demonstrated that the DCPD has played the vital role in the formation of metabolic, non-metabolic stones, bones and teeth (Sivakumar *et al*. 1998).

In reaction solutions both with and without adding mulberry leaf extract at pH of 7 and above, only single-phase HA was observed, and DCPD as well as DCPA peaks were not detected. Some authors have also reported the precipitation of calcium phosphate phases instead of HA at below pH 9 (Afshar *et al*. 2003, Wang *et al*. 2010, Girija *et al*. 2012). At lower pH levels, DCPA and DCPD become more stable in comparison to HA because of the solubility relationship for calcium phosphates (Bohner 2000). According to Sadat-Shojai *et al*. (2012), acting as an intermediate phase during the synthesis of HA under low pHs, DCPD or DCPA must first grow at non-alkaline pH. In an early work (van Kemenade and de Bruyn 1987), at pH of 7.4 and above, crystalline HA is the most stable calcium phosphate. A large source of OH^- groups and ion driving force are the key factors to forming HA crystal (Zhang *et al*. 2011). Cox *et al*. (2014) reported that it is necessary to control and maintain an alkaline pH above 10 when using calcium nitrate tetrahydrate ($Ca(NO_3)_2•4H_2O$) and ammonium phosphate dibasic ($(NH_4)_2HPO_4$) as initial reagents to form HA crystals. Using the same initial reagents as above, Wang *et al*. (2010) also acquired similar results, demonstrating that phase pure HA was identified at pH 10. In this work, phase pure HA could be precipitated at the range of pH 7 to 14 at room temperature using eggshell as the Ca source.

Moreover, detailed investigations on the diffractograms of pure HA in both Figs. 1(a) and (b) revealed that these patterns did not much differ from each other, except in peak broadening and peak intensity, indicating differences in crystallinity and crystallite size. It may mean that although the absence or presence of mulberry leaf extract did not affect the phase purity of HA samples synthesized under different pH values, the samples prepared using mulberry leaf extract had slightly higher crystallinity. Note that this crystallographic structure of low crystallinity and small crystallite sizes is more similar to natural bone mineral. The poorly crystalline HA structure is expected to be more active in metabolic activity than the perfect crystalline structure which is considered to be nonsoluble in physiological environment (Kim *et al*. 2000).

The crystallite sizes of the synthesized HA particles were calculated using the characteristic peaks by Scherrer formula. The result showed that average crystallite sizes decreased gradually as the solution pH levels increased for samples with and without adding mulberry leaf extract, as shown in Table 1. Cox *et al.* (2014) asserted that with increasing the pH level of solution, supersaturation is decreased, resulting in a reduction of subsequent crystal nucleation and growth. The crystallite sizes in the obtained HA powders was around 18.5-29.1 nm for the control samples, and 11.8-14.6 nm for the counterpart samples prepared using mulberry leaf extract. Kamalanathan *et al.* (2014) reported that the crystallite size of HA derived from eggshells as a calcium precursor by precipitation method at a pH level greater than 10.5 was about 35.3 nm, which was greater than that made in the current study. Note that, the crystallite sizes of the HA samples obviously decreased when adding mulberry leaf extract as a template, which is also smaller than that obtained by microwave irradiation route with crystallite sizes in the range of 21-27 nm (Krishna *et al.* 2007, Siddharthan *et al.* 2009). Sadjadi *et al.* (2010) investigated the synthesis of bone-like HA nanorods in wheat starch matrix as a template agent via a biomimetic process. Their results also showed that average crystallite sizes are slightly decreased by using more template of starch.

The templates containing polar functional groups such as COOH and OH are useful components in the formation of nano-sized HA because these ionizable side groups provide a greater affinity to positive calcium ions and the nucleation of HA crystals in the solution (Mollazadeh *et al*. 2007, Wang *et al*. 2009). In other words, calcium ions easily dispersed in a solution at the molecular level because of the interaction within the template and could form the HA nanoparticles (Son and Kim 2013). Therefore, the HA synthesized by adding mulberry leaf extract in this experiment has greater crystallinity and smaller crystallite sizes.

Table 1 The crystallinity, crystallite size and Ca/P ratio of HA synthesized using mulberry leaf extract by aqueous precipitation at room temperature under different pH values. The HA prepared without using mulberry leaf extract was used as a control

		pH 4	pH 7	pH 10	pH 14
Crystallinity, X_c (%)	Control	–	22.2	17.0	23.2
	Mulberry leaf	–	25.4	22.3	23.3
Crystallite size, X_s (nm)	Control	–	29.1	21.5	18.5
	Mulberry leaf	–	14.6	14.3	11.8
Ca/P ratio	Control	0.86±0.07	1.22±0.02	1.41±0.03	1.47±0.03
	Mulberry leaf	0.93±0.02	1.25±0.05	1.50±0.08	1.51±0.04

3.2 Morphology and characterization

The SEM morphologies of the HA particles prepared in the absence and presence of mulberry leaf extract at pH 4, 7, 10 and 14 are shown in Figs. 2(a) and (b), respectively. At pH 4, Fig. 2(a) shows that the DCPD+DCPA particles synthesized at pH 4 without adding mulberry leaf extract have flake-shape structure, while Fig. 2(b) presents that the particles prepared with adding mulberry leaf extract are irregular-shaped DCPD. The morphologies of the HA particles prepared in the absence and presence of mulberry leaf extract at pH 7 and above are also shown in Figs. 2(a) and (b), respectively. Note that, a switch from micrometric particles to nanometric ones suddenly occurred through an increase in pH from 4 to 7. At pH 7, the HA particles exhibited rod-like particle agglomerates with a size of below 100 nm. The agglomeration behavior observed by SEM can be linked with high particle energy associated with nano-sized crystallites causing them to clump together. With increasing pH level from 7 to 14, the particle sizes of the HA gradually decreased, as shown in both Figs. 2(a) and (b). The nanoparticles synthesized at stronger alkaline conditions (pH 14) were short rod shape or close to spherical in shape and less than 50 nm in size. According to the literature (Sadat-Shojai *et al*. 2012), the crystallites can grow to form spherical nanoparticles or at most very short nanorods at high pH value. In the present study, the spherical form was more significant in the sample prepared in the presence of mulberry leaf extract. This observation suggests that the presence of mulberry leaf extract has influence on the morphology of the product. Based on the author's knowledge, this type of nano-HA rod-like or spherical shape structure by mulberry leaf extract addition with precipitation method has never been reported before.

To further verify the formation of nano-HA particles, EDS analysis were applied to characterize their chemical composition. Fig. 3 shows the EDS spectra of the calcium phosphate synthesized with and without adding mulberry leaf extract under different pH values. As expected, EDS spectra showed that the main elements of the final product were Ca, P, C and O. The Ca/P atomic ratio is much lower than that of stoichiometric HA, as shown in Table 1. The negative deviation from the stoichiometric value (1.67) can be ascribed to the presence of calcium-deficient structures. The calcium-deficient HA can have a Ca/P ratio as low as 1.5 (Dorozhkin and Epple 2002), which is very close to that of HA prepared at higher pH levels in the presence of mulberry leaf extract. A small amount of C in the EDS spectra confirms the presence of carbonate group in the samples, which will be discussed in the following section.

Chicken eggshells contain trace elements, such as Mg and Sr, which are also found in human

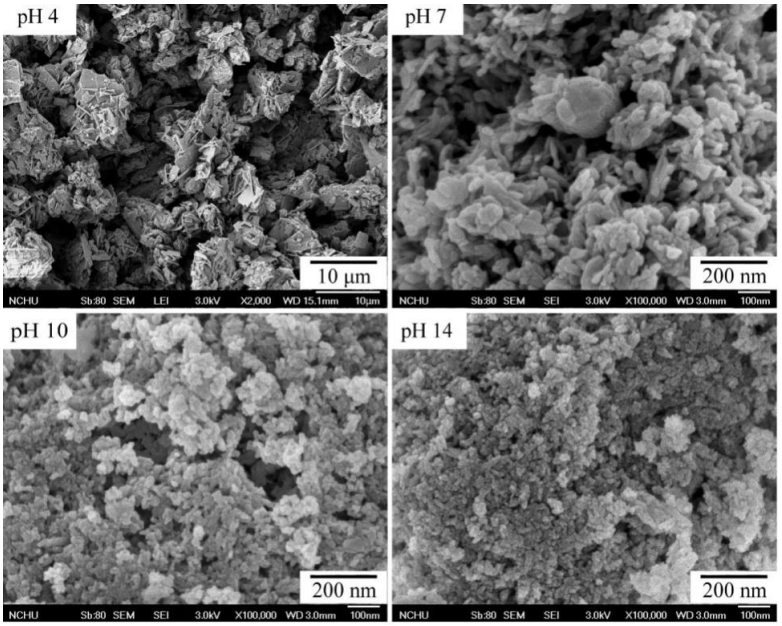

(a) Without adding mulberry leaf extract

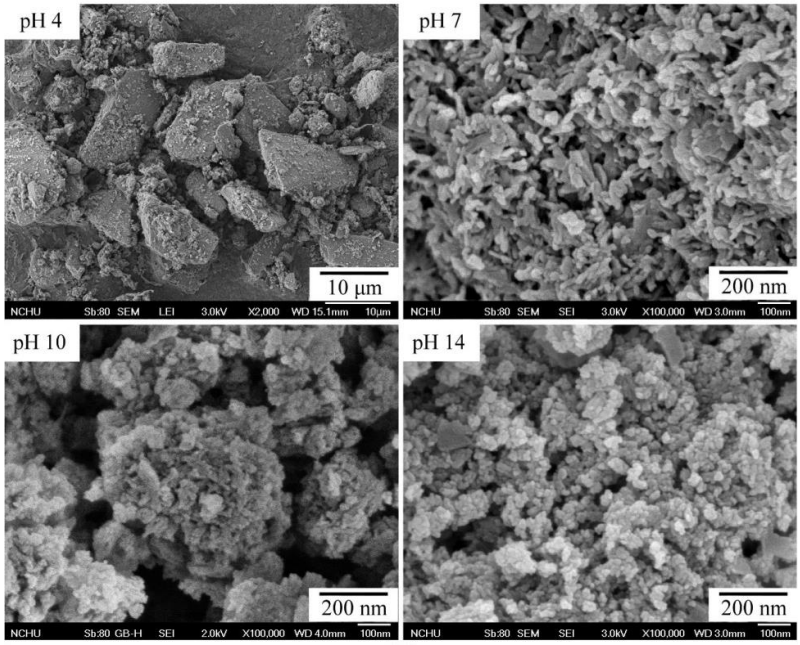

(b) With adding mulberry leaf extract

Fig. 2 SEM images of the synthesized powders with and without adding mulberry leaf extract by aqueous precipitation at room temperature under different pH values

bone. The natural biological origin of eggshells results in produced HA with a composition similar to that of human bone, with considerable benefits to overall physiological function following

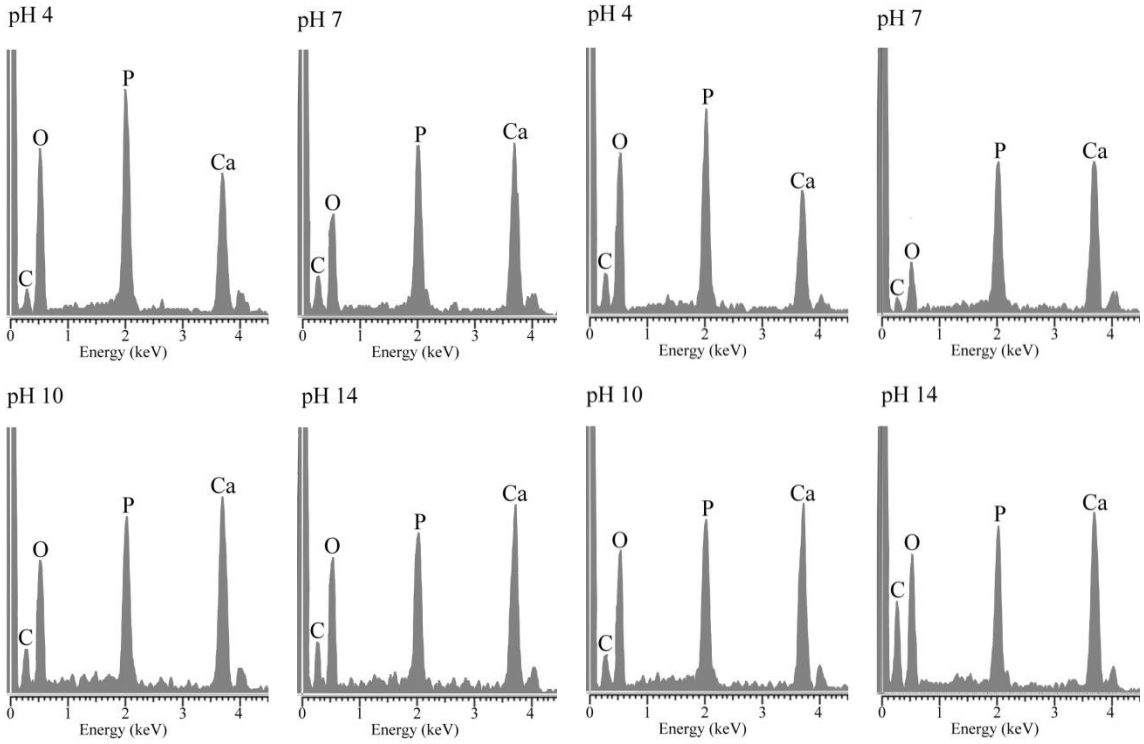

(a) Without adding mulberry leaf extract (b) With adding mulberry leaf extract

Fig. 3 EDS analyses of the synthesized powders with and without adding mulberry leaf extract by aqueous precipitation under different pH values

implantation (Göller *et al*. 2005, Siddharthan *et al*. 2009). The measurements of elemental composition by the ICP-AES method showed the presence of Ca (31.2 wt%), P (14.7 wt%), Mg (0.329 wt%) and Sr (0.038 wt%) in the synthesized HA using mulberry leaf extract after 24 h at pH 10. These elemental substitutions play an important role in bone formation. Magnesium (Mg) has been proved to influence bone mineral metabolism, formation and crystallization processes (Rude *et al*. 2009). In addition, because strontium (Sr) is chemically closely related to calcium (Ca) (Li *et al*. 2007), it is easily introduced as a natural substitute for calcium in HA. There has been increasing awareness of the biological role of Sr, indicating that it could improve the bone strength and provide benefits in the treatment of osteoporosis (Dahl *et al*. 2001).

3.3 Fourier transform infrared analysis

Fig. 4 shows FT-IR spectra of synthesized particles with and without adding mulberry leaf extract as a template under different pH values. At pH 4, in the FT-IR spectra of Figs. 4(a) and (b), the absorption band or a weakly expressed shoulder at around 787 and 1124 cm^{-1} could be due to HPO_4^{2-} group of DCPD or DCPD/DCPA (Baskar *et al*. 2011). At pH 7 and above conditions, the bands assigned to OH^-, PO_4^{3-}, CO_3^{2-} and H_2O are present. The band positions for the OH^- group are at 704, 3742, and 3854 cm^{-1}. The bands for the PO_4^{3-} and CO_3^{2-} groups in the synthetic carbonated HA can be clearly identified. The band observed at 1059 cm^{-1} belongs to the PO_4^{3-}

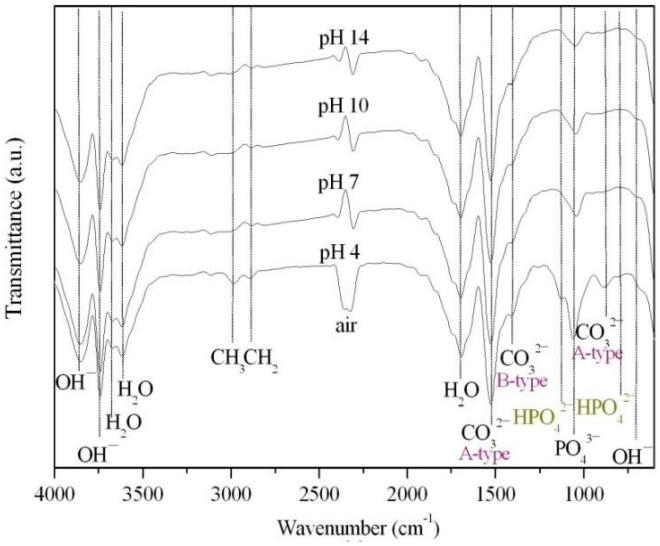

(a) Without adding mulberry leaf extract

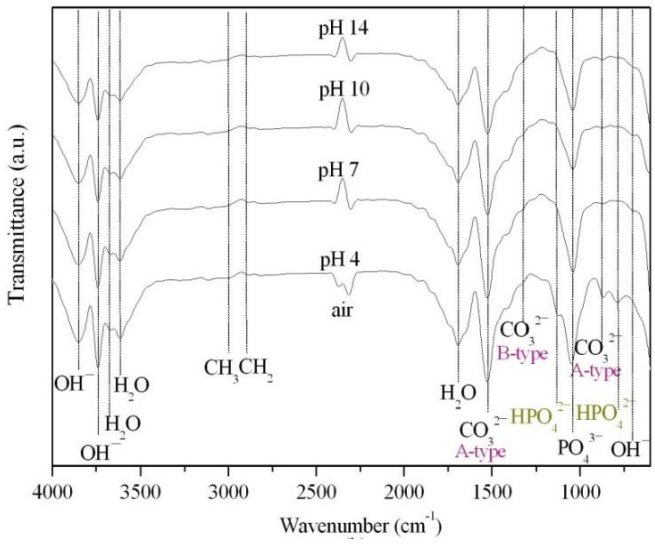

(b) With adding mulberry leaf extract

Fig. 4 FT-IR spectra of the synthesized powders with and without adding mulberry leaf extract by aqueous precipitation at room temperature under different pH values

group. The band positions for the CO_3^{2-} group are at 880, 1406, and 1527 cm^{-1}, which suggest that the powder may have carbonate-substituted HA structure. The CO_3^{2-} ions generated from CO_2 in the reaction solution can substitute OH^- (A-type) or PO_4^{3-} (B-type) in the crystal lattice (Xiao *et al*. 2008). In the present study, the peak at 1406 cm^{-1} were characteristic for B-type carbonate-containing HA, while A-type carbonate were characterized by the peak at 1527 cm^{-1}. Non-stoichiometric carbonated HA is the main mineral components of human and animal hard tissues, which are increasingly used as biocompatible materials for medical uses (Ivanova *et al*. 2001).

4. Conclusions

The current research provides an environmentally beneficial and cost effective method of producing nano-sized carbonated HA powders utilizing an eggshell waste and adding mulberry leaf extract as a template through aqueous precipitation method under different pH values. Our results indicate the following important points:

• At the condition of pH 4, DCPD or DCPA/DCPD phase was observed. At the pH of 7 and above, only one phase of HA were synthesized in reaction solutions both with and without adding mulberry leaf extract.

• Although the absence or presence of mulberry leaf extract did not affect the phase purity of HA samples synthesized under different pH values, the samples prepared using mulberry leaf extract had slightly higher crystallinity.

• The crystallite sizes in the obtained HA powders was around 18.5-29.1 nm for the control samples, and 11.8-14.6 nm for the counterpart samples prepared using mulberry leaf extract. The crystallite sizes of the HA samples obviously decreased when adding mulberry leaf extract as a template, while they decreased gradually as the solution pH levels increased.

• With increasing pH level from 7 to 14, the particle sizes of HA gradually decreased. The HA particles exhibited rod-like particle agglomerates at pH 7, while short rod or spherical shape at pH 14. Especially, the spherical form was more significant in the sample prepared in the presence of mulberry leaf extract.

• The elemental compositions evaluated by the ICP-AES showed the presence of Ca, P, Mg and Sr in the HA synthesized at pH 10 with adding mulberry leaf extract.

• At pH 7 and above conditions, the bands assigned to OH^-, PO_4^{3-}, CO_3^{2-} and H_2O are present. The HA nanoparticles synthesized in the present study can be corresponded to the A- and B-type carbonated structures. All HA powders synthesized in the absence and presence of mulberry leaf extract have similar FT-IR spectra.

Acknowledgments

The authors acknowledge the partial financial support of Ministry of Science and Technology of Taiwan (MOST 105-2218-E-390-002; 106-2218-E-390-001; 107-2218-E-390-001; 107-2218-E-390-007).

References

Afshar, A., Ghorbani, M., Ehsani, N., Saeri, M.R. and Sorrell, C.C. (2003), "Some important factors in the wet precipitation process of hydroxyapatite", *Mater. Des.*, **24**(3), 197-202.

Baskar, D., Balu, R. and Kumar, T.S.S. (2011), "Mineralization of pristine chitosan film through biomimetic process", *Int. J. Biol. Macromol.*, **49**(3), 385-389.

Best, S.M., Porter, A.E., Thian, E.S. and Huang, J. (2008), "Bioceramics: Past, present and for the future", *J. Eur. Ceram. Soc.*, **28**(7), 1319-1327.

Bohner, M. (2000), "Calcium orthophosphates in medicine: From ceramics to calcium phosphate cements", *Injur.*, **31**, D37-D47.

Boutinguiza, M., Pou, J., Comesaña, R., Lusquiños, F., De Carlos, A. and León, B. (2012), "Biological hydroxyapatite obtained from fish bones", *Mater. Sci. Eng. C*, **32**(3), 478-486.

Cox, S.C., Jamshidi, P., Grover, L.M. and Mallick, K.K. (2014), "Low temperature aqueous precipitation of needle-like nanophase hydroxyapatite", *J. Mater. Sci. Mater. Med.*, **25**(1), 37-46.

Dahl, S.G., Allain, P., Marie, P.J., Mauras, Y., Boivin, G., Ammann, P., Tsouderos, Y., Delmas, P.D. and Christiansen, C. (2001), "Incorporation and distribution of strontium in bone", *Bone*, **28**(4), 446-453.

Deng, Y., Sun, Y., Chen, X., Zhu, P. and Wei, S. (2013), "Biomimetic synthesis and biocompatibility evaluation of carbonated apatites template-mediated by heparin", *Mater. Sci. Eng. C*, **33**(5), 2905-2913.

Dorozhkin, S.V. and Epple, M. (2002), "Biological and medical significance of calcium phosphates", *Angew. Chem. Int. Ed.*, **41**(17), 3130-3146.

Fathia, M.H., Hanifia, A. and Mortazavi, V. (2008), "Preparation and bioactivity evaluation of bone-like hydroxyapatite nanopowder", *J. Mater. Proc. Technol.*, **202**(1-3), 536-542.

Girija, E.K., Suresh Kumar, G., Thamizhavel, A., Yokogawa, Y. and Narayana Kalkura, S. (2012), "Role of material processing on the thermal stability and sinterability of nanocrystalline hydroxyapatite", *Powd. Technol.*, **225**, 190-195.

Göller, G., Oktar, F.N., Agathopoulos, S., Tulyaganov, D.U., Ferreira, J.M.F., Kayali, E.S. and Peker, I. (2005), "The influence of sintering temperature on mechanical and microstructural properties of bovine hydroxyapatite", *Key Eng. Mater.*, **284**, 325-328.

Habib, F., Alam, S., Zahra, N., Irfan, M. and Iqbal, W. (2012), "Synthesis route and characterization of hydroxyapatite powder prepared from waste egg shells", *J. Chem. Soc. Pakist.*, **34**(3), 584-588.

Han, Y., Xu, K., Montay, G., Fu, T. and Lu, J. (2002), "Evaluation of nanostructured carbonated hydroxyapatite coatings formed by a hybrid process of plasma spraying and hydrothermal synthesis", *J. Biomed. Mater. Res.*, **60**(4), 511-516.

Ho, W.F., Hsu, H.C., Hsu, S.K., Hung, C.W. and Wu, S.C. (2013), "Calcium phosphate bioceramics synthesized from eggshell powders through a solid state reaction", *Ceram. Inter.*, **39**(6), 6467-6473.

Ivanova, T.I., Frank-Kamenetskaya, O.V., Kol'tsov, A.B. and Ugolkov, V.L. (2001), "Crystal structure of calcium-deficient carbonated hydroxyapatite: thermal decomposition", *J. Sol. State Chem.*, **160**(2), 340-349.

Kamalanathan, P., Ramesh, S., Bang, L.T., Niakan, A., Tan, C.Y., Purbolaksono, J., Chandran, H. and Teng, W.D. (2014), "Synthesis and sintering of hydroxyapatite derived from eggshells as a calcium precursor", *Ceram. Inter.*, **40**(10), 16349-16359.

Kim, H.M., Kim, Y., Park, S.J., Rey, C., Lee, H.M., Gimcher, M.J. and Ko, J.S. (2000), "Thin film of low-crystalline calcium phosphate apatite formed at low temperature", *Biomater.*, **21**(11), 1129-1134.

Krishna, D.S.R., Siddharthan, A., Seshadri, S.K. and Kumar, T.S.S. (2007), "A novel route for synthesis of nanocrystalline hydroxyapatite from eggshell waste", *J. Mater. Sci. Mater. Med.*, **18**(9), 1735-1743.

Landi, E., Tampieri, A., Celotti, G. and Sprio, S. (2000), "Densification behavior and mechanisms of synthetic hydroxyapatites", *J. Eur. Ceram. Soc.*, **20**(14-15), 2377-2387.

Li, Z.Y., Lam, W.M., Yang, C., Xu, B., Ni, G.X., Abbah, S.A., Cheung, K.M.C., Luk, K.D.K. and Lu, W.W. (2007), "Chemical composition, crystal size and lattice structural changes after incorporation of strontium into biomimetic apatite", *Biomater.*, **28**(7), 1452-1460.

Liu, D., Troczynski, T. and Tseng, W.J. (2001), "Water-based sol-gel synthesis of hydroxyapatite: Process development", *Biomater.*, **22**(13), 1721-1730.

Liu, J., Ye, X., Wang, H., Zhu, M., Wang, B. and Yan, H. (2003), "The influence of pH and temperature on the morphology of hydroxyapatite synthesized by hydrothermal method", *Ceram. Int.*, **29**(6), 629-633.

Matsuura, A., Kubo, T., Doi, K., Hayashi, K., Morita, K., Yokota, R., Hayashi, H., Hirata, I., Okazaki, M. and Akagawa, Y. (2009), "Bone formation ability of carbonate apatite-collagen scaffolds with different carbonate contents", *Dent. Mater. J.*, **28**(2), 234-242.

Mollazadeh, S., Javadpour, J. and Khavandi, A. (2007), "In situ synthesis and characterization of nano-size hydroxyapatite in poly (vinyl alcohol) matrix", *Ceram. Int.*, **33**(8), 1579-1583.

Neira, I.S., Kolen'ko, Y.V., Lebedev, O.I., Van Tendeloo, G., Gupta, H.S., Guitian, F. and Yoshimura, M. (2009), "An effective morphology control of hydroxyapatite crystals via hydrothermal synthesis", *Cryst. Grow. Des.*, **9**(1), 466-474.

Rude, R.K., Singer, F.R. and Gruber, H.E. (2009), "Skeletal and hormonal effects of magnesium

deficiency", *J. Am. Coll. Nutr.*, **28**(2), 131-141.
Sadat-Shojai, M., Khorasani, M.T. and Jamshidi, A. (2012), "Hydrothermal processing of hydroxyapatite nanoparticles-a Taguchi experimental design approach", *J. Cryst. Grow.*, **361**, 73-84.
Sadjadi, M.S., Meskinfam, M., Sadeghi, B., Jazdarreh, H. and Zare, K. (2010), "In situ biomimetic synthesis, characterization and in vitro investigation of bone-like nanohydroxyapatite in starch matrix", *Mater. Chem. Phys.*, **124**(1), 217-222.
Siddharthan, A., Kumar, T.S. and Seshadri, S.K. (2009), "Synthesis and characterization of nanocrystalline apatites from eggshells at different Ca/P ratios", *Biomed. Mater.*, **4**(4), 045010.
Sivakumar, G.R., Girija, E.K., Narayanakalkura, S. and Subramanian, C. (1998), "Crystallization and characterization of calcium phosphates: Brushite and monetite", *Cryst. Res. Technol.*, **33**(2), 197-205.
Son, K.D. and Kim, Y.J. (2013), "Morphological structure and characteristics of hydroxyapatite/*β*-cyclodextrin composite nanoparticles synthesized at different conditions", *Mater. Sci. Eng. C*, **33**(1), 499-506.
Tadic, D., Peters, F. and Epple, M. (2002), "Continuous synthesis of amorphous apatites", *Biomater.*, **23**(12), 2553-2559.
Tas, A.C. (2000), "Synthesis of biomimetic Ca-hydroxyapatite powders at 37°C in synthetic body fluids", *Biomater.*, **21**(14), 1429-1438.
Van Kemenade, M.J.J.M. and De Bruyn, P.L. (1987), "A kinetic study of precipitation from supersaturated calcium phosphate solutions", *J. Colloid Interf. Sci.*, **118**(2), 564-585.
Vega, E.D., Pedregosa, J.C., Narda, G.E. and Morando, P.J. (2003), "Removal of oxovanadium (IV) from aqueous solutions by using commercial crystalline calcium hydroxyapatite", *Water Res.*, **37**(8), 1776-1782.
Wang, P., Li, C., Gong, H., Jiang, X., Wang, H. and Li, K. (2010), "Effects of synthesis conditions on the morphology of hydroxyapatite nanoparticles produced by wet chemical process", *Powd. Technol.*, **203**(2), 315-321.
Wang, P., Yook, S.W., Jun, S.H., Li, Y.L., Kim, M., Kim, H.E. and Koh, Y.H. (2009), "Synthesis of nanoporous calcium phosphate spheres using poly (acrylic acid) as a structuring unit", *Mater. Lett.*, **63**(13-14), 1207-1209.
Wu, S.C., Hsu, H.C., Wu, Y.N. and Ho, W.F. (2011), "Hydroxyapatite synthesized from oyster shell powders by ball milling and heat treatment", *Mater. Character.*, **62**(12), 1180-1187.
Wu, S.C., Tsou, H.K., Hsu, H.C., Hsu, S.K., Liou, S.P. and Ho, W.F. (2013), "A hydrothermal synthesis of eggshell and fruit waste extract to produce nanosized hydroxyapatite", *Ceram. Inter.*, **39**(7), 8183-8188.
Xiao, X.F., Liu, R.F. and Gao, Y.J. (2008), "Hydrothermal preparation of nanocarbonated hydroxyapatite crystallites", *Mater. Sci. Technol.*, **24**(10), 1199-1203.
Zhang, Y., Liu, Y., Ji, X., Banks, C.E. and Song, J. (2011), "Flower-like agglomerates of hydroxyapatite crystals formed on an egg-shell membrane", *Colloids Surf. B*, **82**(2), 490-496.

CC